引用格式：ZHU Jintao, SHI Jingzhan, ZHU Dan, et al. Phase Noise Suppression System for Microwave Photonic FMCW Radar Based on Deskew Filtering[J]. Acta Photonica Sinica, 2026, 55(3):0355113
朱锦韬,史经展,朱丹,等.基于去偏斜滤波的微波光子调频连续波雷达相位噪声抑制系统[J].光子学报,2026,55(3):0355113

基于去偏斜滤波的微波光子调频连续波雷达相位噪声抑制系统

朱锦韬,史经展,朱丹,刘强,林冬冬,张娜,高彬栋,汪弋平
(南京师范大学 计算机与电子信息学院 大规模复杂系统数值模拟教育部重点实验室,南京 210023)

摘　要:提出并验证了一种基于去偏斜滤波的微波光子调频连续波雷达相位噪声抑制系统。该系统采用光四倍频结构,以提升雷达的距离分辨率。引入参考延时和混频支路,获取参考去斜信号,并结合去偏斜滤波算法,对回波去斜信号中的相位抖动进行有效补偿。实验结果表明,该系统成功实现了基带线性调频信号的四倍频,显著扩展了雷达信号的带宽。在相位噪声补偿后,回波去斜信号的半周期稳定性提高了3.6倍,相位噪声得到了有效抑制。同时,距离像中目标能量更加集中,雷达的测距精度和分辨率显著提升,从而验证了去偏斜滤波方法在抑制微波光子雷达相位噪声方面的有效性。

关键词:微波光子倍频;调频连续波雷达;相位噪声;去偏斜滤波;相位噪声补偿
中图分类号:TN015　　**文献标识码**:A　　**doi**:10.3788/gzxb20265503.0355113

0　引言

调频连续波(Frequency Modulated Continuous Wave, FMCW)雷达通过发射频率随时间线性变化的信号,利用回波信号与发射信号之间的频率差来实现对目标距离和速度的高精度测量。其优势在于具备高分辨率[1]、低功耗以及较强的抗干扰能力[2],广泛应用于军事侦察、精确制导、无人驾驶和气象监测等领域。随着对雷达系统更高分辨率[3,4]和更远探测距离[1]需求的不断提升,传统微波电子雷达因受“电子瓶颈”的限制,在宽带信号的产生、处理与控制方面面临带宽受限、性能提升困难[5]的问题。为解决这一难题,微波光子雷达应运而生。该技术结合了光子学与电子学的优势,利用光子技术实现高载频[6]、大带宽[7]信号的生成与处理,从而突破了传统电子雷达的性能限制。

根据FMCW信号的生成方式及回波接收处理方式的不同,微波光子FMCW雷达系统主要可分为四类:光频时映射生成与光模数转换接收[8]、光注入半导体激光器生成与光去斜接收[9]、光倍频生成与光去斜接收[10]、光数模转换生成与光去斜接收[11]。其中,基于光倍频生成与光去斜接收架构的微波光子FMCW雷达,利用微波光子倍频技术生成高频宽带的线性调频信号,并结合微波光子混频技术对回波信号进行去斜处理。该架构凭借其大带宽和实现结构相对简单的优点,获得了广泛关注。已有报道显示[12],采用该架构的微波光子FMCW雷达发射信号带宽达到18 GHz,距离分辨率达到8.3 mm。此外,基于该架构的相控阵雷达[13]、多载波雷达[14]以及多输入多输出(Multiple Input Multiple Output, MIMO)雷达[15]等新型雷达系统相继出现,进一步展示了光倍频生成与光去斜接收架构在FMCW雷达中的优异性能。

对于FMCW雷达,FMCW信号的相位噪声会损伤雷达性能。当FMCW信号含有相位噪声时,去斜信

基金项目:国家自然科学基金(62575140,62101269,62501291,62405139,62401268,62505139),中国科协青年人才托举工程(2022QNRC001),雷达成像与微波光子技术教育部重点实验室(南京航空航天大学)开放课题(NJ20210007),江苏省高校自然科学基金面上项目(24KJB510014)
第一作者:朱锦韬,232212038@njnu.edu.cn
通讯作者:史经展,shijz@nnu.edu.cn
收稿日期:2025-08-02;**录用日期**:2025-09-11

号的频率(相位)随时间变化,频谱被展宽。首先,去斜信号的频率或相位是FMCW雷达实现距离、方位和速度测量的主要依据,因此相位噪声引起的频率(相位)时变效应会损伤雷达测量精度;其次,去斜信号的频谱宽度直接决定了FMCW雷达的测距分辨率,因此相位噪声引起的频谱展宽效应会损伤雷达测距分辨率;此外,频谱展宽效应会导致小目标被淹没在干扰杂波的频谱下,因此相位噪声会损伤雷达抗干扰能力。特别地,对于基于光倍频生成与光去斜接收架构的微波光子FMCW雷达,虽然微波光子倍频技术能够提升雷达信号带宽和距离分辨率,但倍频过程本身会导致信号相位噪声恶化。当倍频数为n时,倍频信号的相位噪声通常会恶化$20\lg n$ dB[16]。此外,微波光子倍频与去斜过程中涉及电-光转换、信号放大以及光-电探测等有源模块,这些环节也可能进一步加剧去斜信号的相位噪声[17]。综上所述,相位噪声已成为制约微波光子FMCW雷达充分发挥其宽带优势的关键因素。显然,为满足各类应用对雷达日益增长的探测精度、分辨率和抗干扰能力需求,FMCW雷达的相位噪声亟需得到抑制。

针对FMCW雷达的相位噪声抑制技术主要分为两种:一是生成具有低相位噪声的FMCW信号;二是通过数字信号后处理设计算法对相位噪声进行补偿。典型的后处理方法包括去偏斜滤波法、等相位间隔采样法[18]等。其中,去偏斜滤波法的核心思想是构建一条参考延时支路,并根据参考支路接收信号的相位噪声来重构并补偿实际回波信号中的相位噪声。由于该方法易于与现有系统集成且具备良好的实时性,已被广泛应用于数字通信[19]、图像处理[20]、雷达信号处理[21]和光纤传感[22]等领域。

由于微波光子FMCW雷达的研究起步较晚,关于其相位噪声抑制的报道较少,且现有研究多集中于第一种方法,即通过光子技术生成低相位噪声的FMCW信号,包括光电振荡器[23-27](Optoelectronic Oscillator, OEO)、光分频技术[14,28]和光相干外差技术[29]。尽管光子技术能够有效降低FMCW信号源的相位噪声,从而实现相位噪声的抑制,但这种方法也带来了系统结构复杂化的问题,显著提高了制造成本。此外,光生微波系统涉及光电或电光转换过程,而这些转换过程本身可能引入新的相位噪声,从而限制了对相位噪声的改善效果。近期,我们已将等相位间隔采样法应用于微波光子FMCW雷达的相位噪声补偿[18],成功提高了雷达的测距精度。但是,等相位间隔采样法需要精确定位等相位间隔的时刻,要求采集去斜信号的模数转换器(Analog-to-Digital Converter, ADC)具有较高的采样率和精度。

鉴于现有微波光子FMCW雷达相位噪声抑制技术中,光子生成低噪声信号存在系统复杂、成本高及转换过程可能引入新噪声的局限,而等相位间隔采样法对ADC性能要求严苛,本文提出一种基于去偏斜滤波的微波光子FMCW雷达相位噪声补偿方法。该方法创新性地通过新增参考延时和混频支路构建参考信号链路,结合去偏斜滤波算法精准补偿回波去斜信号中的相位抖动,在无需复杂光子生成模块或高精度ADC的情况下,实现对相位噪声的有效抑制。以下将详细阐述该方法的系统原理、实验验证过程及结果分析,以论证其可行性与优越性。

1 系统原理

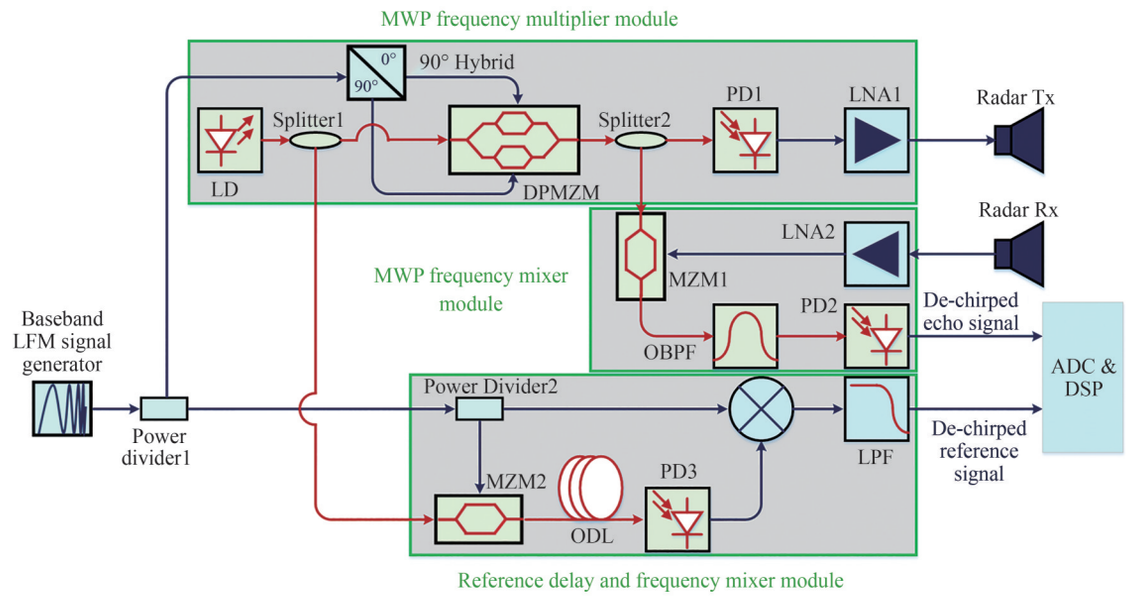
基于去偏斜滤波的微波光子FMCW雷达相位噪声抑制系统如图1所示,在传统光倍频生成与光去斜接收架构的基础上,新增了参考延时和混频支路。这一改进为去偏斜滤波算法提供了必要的参考信号,从而提升系统对相位噪声的抑制能力。

含有相位噪声的基带线性调频(Linear Frequency Modulation, LFM)信号表达式为

$$E_s(t)=A_0\cos\left(2\pi f_0 t+\pi k t^2+e(t)\right) \tag{1}$$

式中,A_0为信号幅度,f_0为信号初始频率,k为LFM信号调谐率,$k=B/T$,B为信号带宽,T为周期,$e(t)$为相位抖动。

基带LFM信号通过功分器被分为两路。其中一路输入至由激光器、90度电桥、双平行马赫-曾德尔调制器(Dual-Parallel Mach-Zehnder Modulator, DPMZM)和光电探测器(Photodetector, PD)组成的微波光子四倍频模块。经过90度耦合器后,基带LFM信号被分为相位相差90度的两路信号,并分别驱动DPMZM内部并行设置的两个子马赫曾德尔调制器(Mach-Zehnder Modulator, MZM)。当两个子MZM偏置于最大传输点,且主MZM加载半波电压V_π时,DPMZM输出的光谱主要由±2阶调制边带组成。DPMZM输出的光信号再次被分为两路。其中一路经光电探测器PD1进行光电转换,生成雷达发射的LFM信号,其频率为



LD: Laser Diode; DPMZM: Dual-Parallel Mach-Zehnder Modulator; MZM: Mach-Zehnder Modulator; PD: Photodetector; LNA: Low Noise Amplifier; OBPF: Optical Bandpass Filter; ODL: Optical Delay Line; LPF: Lowpass Filter; ADC: Analog-to-Digital Converter; DSP: Digital Signal Processor

图1　基于去偏斜滤波的微波光子FMCW雷达相位噪声抑制系统

Fig.1　System for phase noise suppression in MWP FMCW Radar based on deskew filter

$4f_0+4kt$，携带的相位抖动为$4e(t)$。可以看出，与基带LFM信号相比，雷达发射信号的初始频率和带宽均被放大了四倍，但其相位抖动也随之增大。雷达发射信号经天线辐射并经目标反射后获得延时量为τ_d的雷达回波信号，该信号由微波光子混频模块完成去斜接收处理。在偏置于正交点的MZM1中，雷达回波信号对DPMZM输出的另一路光信号进行调制，随后通过光带通滤波器选择+2阶或−2阶调制边带，最终经光电转换得到回波去斜信号，表示为

$$E_e(t)=A_e\cos\left(8\pi f_0\tau_d+8\pi k\tau_d t-4\pi k\tau_d^2+4e(t)-4e(t-\tau_d)\right) \tag{2}$$

式(2)表明，回波去斜信号的频率为$4k\tau_d$，相位抖动为$4e(t)-4e(t-\tau_d)$。对于FMCW雷达而言，目标的距离是根据去斜信号的频率测得的。然而，由于相位抖动的存在，去斜信号的频率会出现偏移和随机波动，从而导致距离测量的准确度和精度下降。

为实现对式(2)所示回波去斜信号中相位抖动的精确补偿，系统通过微波光子延时线对基带LFM信号引入参考延时τ_r，并利用混频器对原始基带LFM信号与延时后的信号进行混频，随后经过低通滤波器处理，从而获得参考去斜信号。需要指出的是，由于原始LFM信号的频率和带宽相对较小，此处的混频过程可采用电混频器完成。由此得到的参考去斜信号表示为

$$E_r(t)=A_r\cos\left(2\pi f_0\tau_r+2\pi k\tau_r t-\pi k\tau_r^2+e(t)-e(t-\tau_r)\right) \tag{3}$$

可以看出，参考去斜信号的频率为$k\tau_r$，相位抖动为$e(t)-e(t-\tau_r)$。

接着，使用ADC采集回波去斜信号和参考去斜信号，并在DSP(Digital Signal Processor，DSP)中利用去偏斜滤波算法对其进行处理。去偏斜滤波算法流程如图2所示。

第一步：将式(2)所示回波去斜信号进行希尔伯特变换得到其复信号，即

$$Z_{e1}(t)=E_e(t)+\mathrm{j}H\left[E_e(t)\right]=A_e\mathrm{e}^{\mathrm{j}2\pi\left(4f_0\tau_d+4k\tau_d t-2k\tau_d^2\right)}\mathrm{e}^{\mathrm{j}\left(4e(t)-4e(t-\tau_d)\right)} \tag{4}$$

式中，$H[\ ]$为希尔伯特变换。$\mathrm{e}^{\mathrm{j}4e(t)}$和$\mathrm{e}^{-\mathrm{j}4e(t-\mathrm{rd})}$分别为与发射信号和回波信号相位抖动相关的相位项，下面利用参考去斜信号对它们进行补偿。

第二步：补偿$\mathrm{e}^{\mathrm{j}4e(t)}$。此步骤的关键在于估计$e(t)$，为此，对式(3)所示参考去斜信号进行希尔伯特变换得到其复信号，即

$$Z_r(t)=E_r(t)+\mathrm{j}H\left[E_r(t)\right]=A_r\mathrm{e}^{\mathrm{j}\left(2\pi f_0\tau_r+2\pi k\tau_r t-\pi k\tau_r^2+e(t)-e(t-\tau_r)\right)} \tag{5}$$

接着，提取该复信号的相角，得到

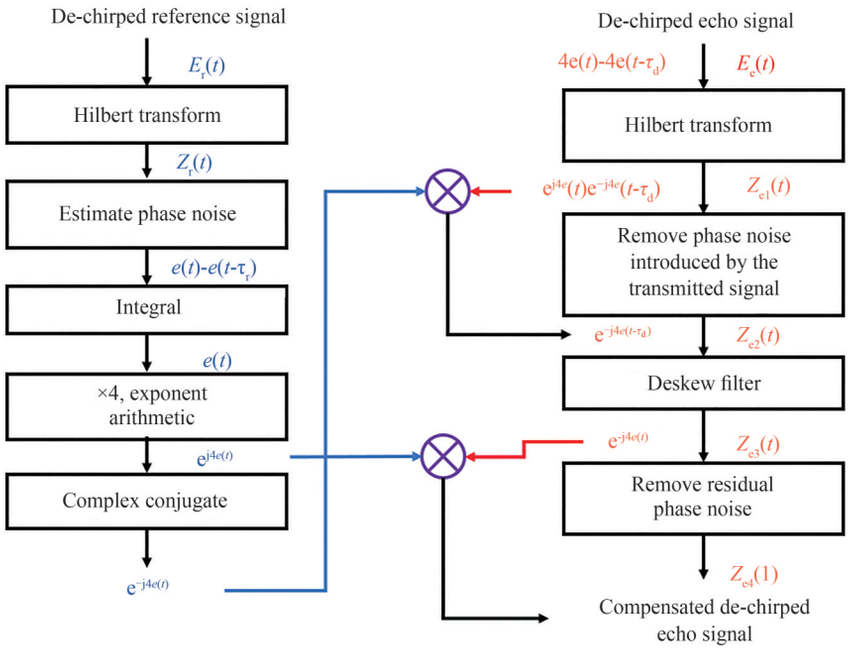


图 2 算法流程

Fig.2 Algorithm flow

$$\theta(t)=\arg\left[Z_r(t)\right]=2\pi f_0\tau_r+2\pi k\tau_r t-\pi k\tau_r^2+e(t)-e(t-\tau_r) \tag{6}$$

由于参考去斜信号中的f_0、k、τ_r均已知，则参考去斜信号中的相位抖动$e(t)-e(t-\tau_r)$为

$$e(t)-e(t-\tau_r)=\theta(t)-\left(2\pi f_0\tau_r+2\pi k\tau_r t-\pi k\tau_r^2\right) \tag{7}$$

根据泰勒级数展开公式，当τ_r较小时，$e(t)-e(t-\tau_r)$近似可表示为$e'(t)\tau_r$。因此，$e(t)$可估计得到

$$e(t)=\int_0^t\frac{e(\mu)-e(\mu-\tau_r)}{\tau_r}\mathrm{d}\mu \tag{8}$$

令$\varphi_e(t)=e^{j4e(t)}$，随后，将式(4)所示复数回波去斜信号乘以$\varphi_e(t)$的共轭$\varphi_e^*(t)$，得到

$$\begin{aligned}Z_{e2}(t)&=Z_{e1}(t)\varphi_e^*(t)\\&=A_e e^{j2\pi\left(4f_0\tau_d+4k\tau_d t-2k\tau_d^2\right)}e^{j4\left(e(t)-e(t-\tau_d)\right)}e^{-j4e(t)}\\&=A_e e^{j2\pi\left(4f_0\tau_d+4k\tau_d t-2k\tau_d^2\right)}\varphi_e^*(t-\tau_d)\end{aligned} \tag{9}$$

可以看出，与发射信号相位抖动相关的项$e^{j4e(t)}$得到补偿。

第三步：补偿$\varphi_e^*(t-\tau_d)$。由于$\varphi_e^*(t-\tau_d)$与延时τ_d有关，无法通过单一的参考信号直接消除所有延时处的噪声项，需要去除相位项$\varphi_e^*(t-\tau_d)$对于τ_d的依赖。为此，采用去偏斜滤波法，引入一个与频率二次方成比例的群延迟，去偏斜滤波器的频域传递函数为$\exp(j\pi f^2/4k)$。当式(9)所示复信号通过去偏斜滤波后，其频谱为

$$\begin{aligned}\mathcal{F}\left[Z_{e3}(t)\right]&=\mathcal{F}\left[Z_{e2}(t)\right]e^{j\frac{\pi f^2}{4k}}\\&=\left\{A_e e^{j2\pi\left(4f_0\tau_d-2k\tau_d^2\right)}\mathcal{F}\left[e^{j2\pi\times 4k\tau_d t}\right]\otimes\mathcal{F}\left[\varphi_e^*(t-\tau_d)\right]\right\}e^{j\frac{\pi f^2}{4k}}\\&=\left\{A_e e^{j2\pi\left(4f_0\tau_d-2k\tau_d^2\right)}\delta\left(f-4k\tau_d\right)\otimes\Psi\left(f\right)e^{-j2\pi f\tau_d}\right\}e^{j\frac{\pi f^2}{4k}}\\&=A_e e^{j2\pi\left(4f_0\tau_d-2k\tau_d^2\right)}\Psi\left(f-4k\tau_d\right)e^{-j2\pi\left(f-4k\tau_d\right)\tau_d}e^{j\frac{\pi f^2}{4k}}\\&=A_e e^{j8\pi f_0\tau_d}e^{j\frac{\pi}{4k}\left(f-4k\tau_d\right)^2}\Psi\left(f-4k\tau_d\right)\\&=A_e e^{j8\pi f_0\tau_d}\delta\left(f-4k\tau_d\right)\otimes\left(e^{j\frac{\pi f^2}{4k}}\Psi\left(f\right)\right)\end{aligned} \tag{10}$$

式中，$\Psi(f)$为$\varphi_e^*(t)$的傅里叶变换。对式(10)所示频谱进行傅里叶反变换，即可得到$Z_{e3}(t)$

$$\begin{aligned} Z_{e3}(t) &= \mathcal{F}^{-1}\left[A_e e^{j8\pi f_0\tau_d}\delta\left(f-4k\tau_d\right)\otimes\left(e^{j\frac{\pi f^2}{4k}}\Psi\left(f\right)\right)\right] \\ &= \mathcal{F}^{-1}\left[A_e e^{j8\pi f_0\tau_d}\delta\left(f-4k\tau_d\right)\right]\mathcal{F}^{-1}\left[e^{j\frac{\pi f^2}{4k}}\Psi\left(f\right)\right] \\ &= A_e e^{j\left(4k\tau_d t+8\pi f_0\tau_d\right)}\left\{\mathcal{F}^{-1}\left[e^{j\frac{\pi f^2}{4k}}\right]\otimes\mathcal{F}^{-1}\left[\Psi\left(f\right)\right]\right\} \\ &= A_e e^{j\left(4k\tau_d t+8\pi f_0\tau_d\right)}\left[q_k(t)\otimes\varphi_e^*(t)\right] \end{aligned} \tag{11}$$

式中，$q_k(t)=\mathcal{F}^{-1}\left[e^{j\frac{\pi f^2}{4k}}\right]=\sqrt{j4k}\,e^{-j4k\pi t^2}$，当$k$的取值满足“$kT^2\gg1$”时，$q_k(t)\approx\delta(t)$[21]，式(11)可以表示为

$$Z_{e3}(t)=A_e e^{j\left(4k\tau_d t+8\pi f_0\tau_d\right)}\varphi_e^*(t) \tag{12}$$

接着，利用前面得到的$\varphi_e(t)$即可实现对$\varphi_e^*(t)$的补偿，即

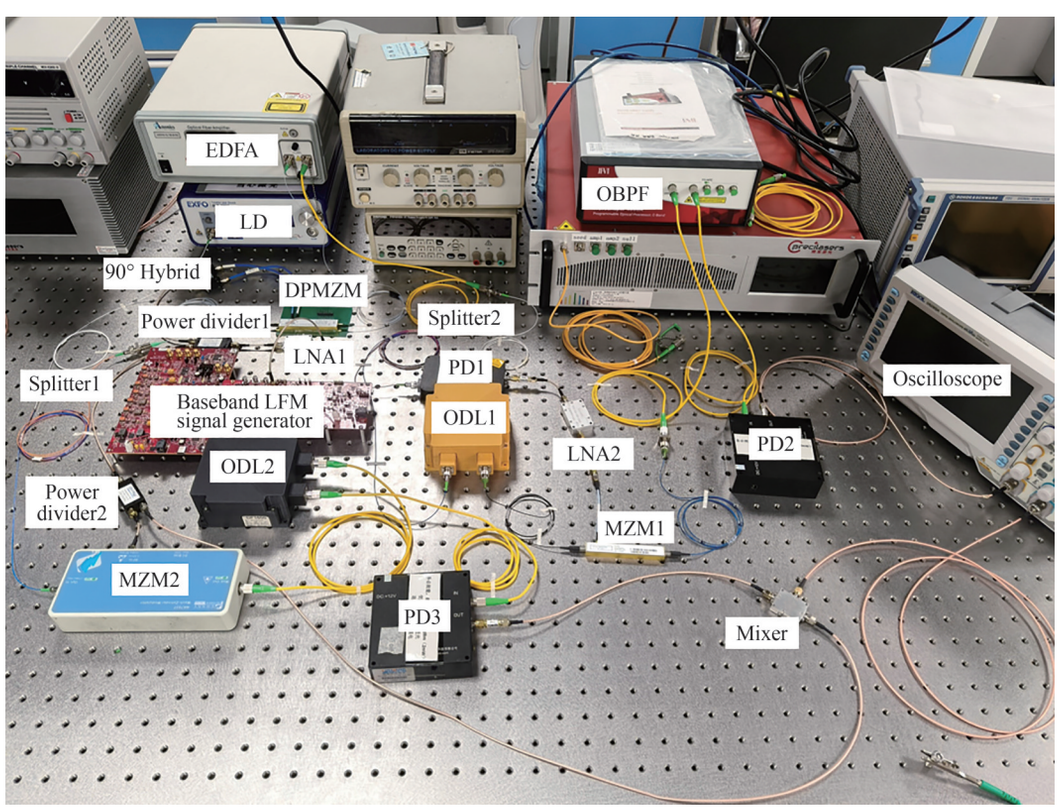
$$Z_{e4}(t)=Z_{e3}(t)\varphi_e(t)=A_e e^{j\left(4k\tau_d t+8\pi f_0\tau_d\right)} \tag{13}$$

式(13)所示信号不再含有相位抖动，其频率值为$4k\tau_d$，为恒定值，说明相位噪声得到了补偿。

2 实验结果

为了验证基于去偏斜滤波的微波光子FMCW雷达相位噪声抑制系统的可行性，搭建了如图3所示的实验装置，主要设备及其参数信息如表1所示。需要说明的是，受实验条件限制，该实验系统中采用了一段延时量约为8 000 ns的光纤延时线来模拟雷达收发机与目标之间的往返传播时延。

首先验证了微波光子四倍频功能。基带LFM信号由矢量信号发生器(TI，AFE7950EVM)生成，设置初始频率为5 GHz，带宽为100 MHz，周期为65.54 μs，对应的啁啾率为1.525 9 MHz/μs，其时频关系如图4(a)所



EDFA: Erbium-doped Fiber Amplifier; OBPF: Optical Bandpass Filter

图3 基于去偏斜滤波的微波光子FMCW雷达相位噪声抑制系统实验装置

Fig.3 Experimental setup of the microwave photonic FMCW radar phase noise suppression system based on deskew filtering

表1 实验所用器件及其参数

Table 1 Devices and their parameters used in the experiment

Device	Manufacturer, version	Specifications
LD	EXFO, FLS-2800	Wavelength: 1 550.12 nm Power: 10 dBm
90° Hybrid	SHW, SHWHB-002001800	Frequency: 2~18 GHz
DPMZM	AFR, 40G-IQ-XT	40 GHz/C+L band/1.85 mm
MZM1	Fujitsu, FTM7937	≥25 GHz/C band/2.92 mm
MZM2	Newkey Photonics, NK7937	≥25 GHz/C band/2.92 mm
ODL1	Newkey Photonics, DF1600	Delay: 8 000 ns
ODL2(reference path)	Newkey Photonics, DF160	Delay: 800 ns
PD1	HLT, PD-M-40-0-1-FA	Bandwidth: 0~40 GHz
PD2	Conquer, PD-20G21442	Bandwidth: 0~20 GHz
PD3	Conquer, PD-20G21442	Bandwidth: 0~20 GHz
Mixer	Marki, IQLMP	Frequency: 1.5~6 GHz
OBPF	Luster, WaveShaper 4000A	Wavelength: 1 528~1 567 nm Resolution bandwidth: 10 GHz
Oscilloscope	RIGOL, DS2302A	Sampling rate: 2 GSa/s

示。基带LFM信号用于驱动双平行马赫-曾德尔调制器(DPMZM),其输出光谱如图4(b)所示。可以看出,DPMZM输出光谱中的奇数阶调制边带和光载波均被抑制,仅保留了±2阶调制边带。该光信号经过光电转换后,得到基带LFM信号的四倍频信号,其频谱如图4(c)所示。从频谱可以看出,四倍频信号的频率范

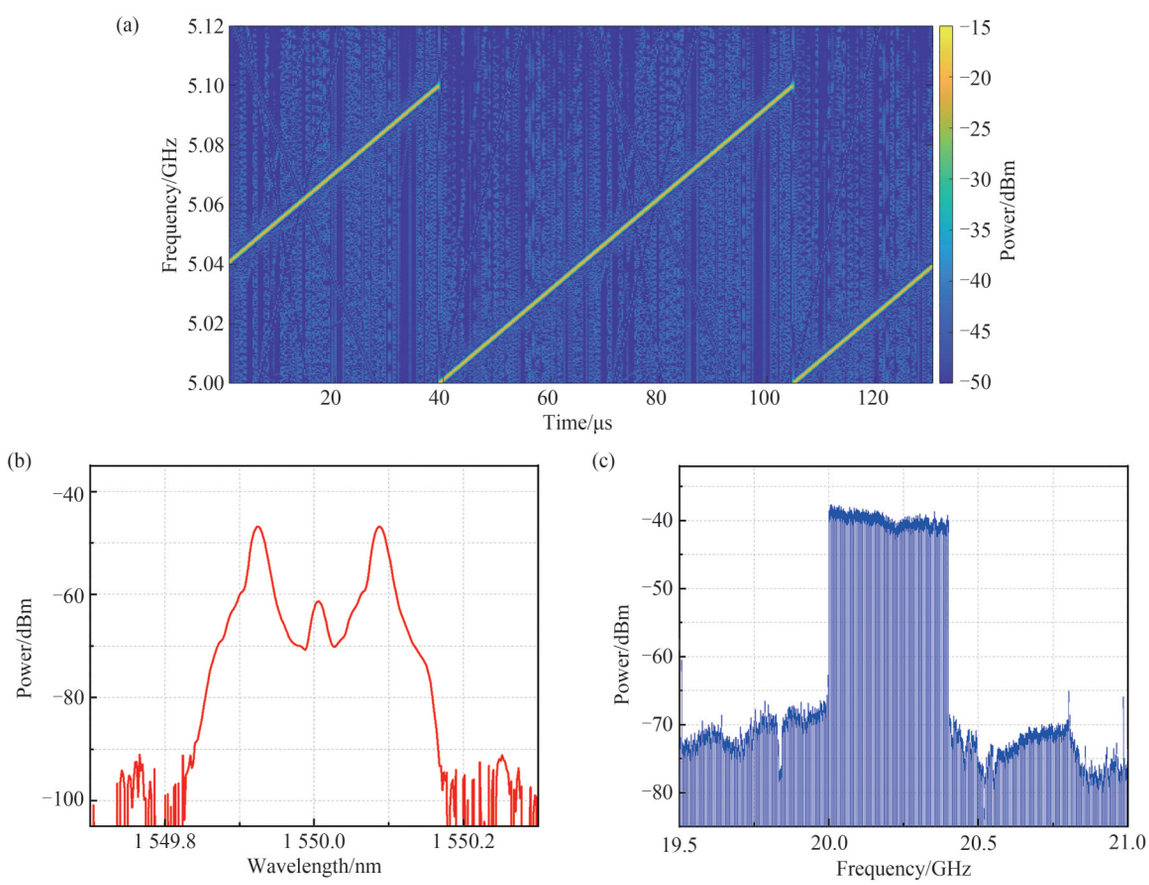


图4 微波光子四倍频功能验证。(a)基带LFM信号时频图;(b)DPMZM输出光谱;(c)四倍频信号频谱

Fig.4 Verification of microwave photonic quadruple-frequency function; (a) Time-frequency diagram of the baseband LFM signal; (b) Output optical spectrum of DPMZM; (c) Spectrum of the quadruple-frequency signal

围为20 GHz至20.4 GHz，相比基带LFM信号，其初始频率和带宽均扩展为原来的四倍。

在设置参考路径时延为800 ns（由光延时线2提供）后，利用实时示波器（Rigol DS2302A）采集并记录参考去斜信号和回波去斜信号的波形。图5(a)展示了0至1.5 μs时间段内的信号波形。随后，依次按照式(5)至式(8)对参考去斜信号进行处理，估计得到的相位抖动如图5(b)所示。最终，分别通过公式(9)和去偏斜滤波器对回波去斜信号中与发射信号和回波信号相位抖动相关的相位项进行补偿，从而获得相位噪声补偿后的回波去斜信号。选取其中一段波形展示如图5(c)所示。可以看出，经过相位噪声补偿后，回波去斜信号的相位相较于补偿前发生了偏移。

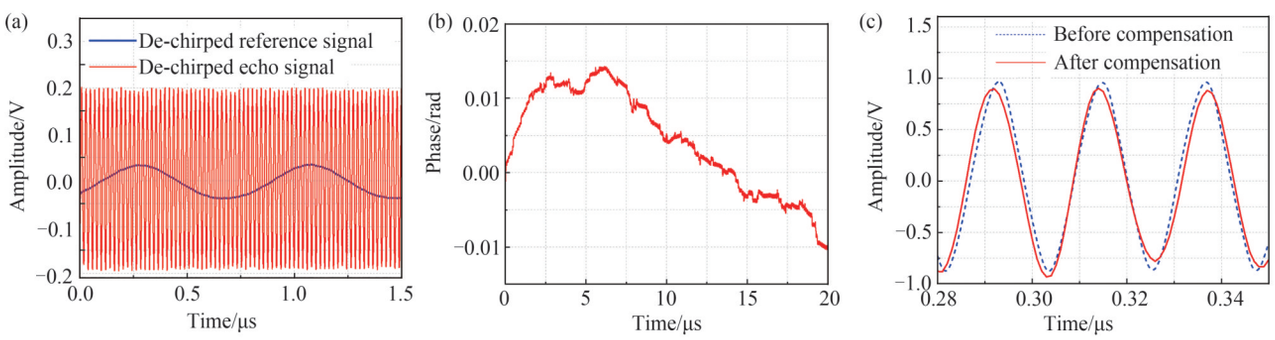


图5　去斜信号与相位抖动估计值的时域波形。(a)参考去斜与回波去斜信号；(b)参考去斜信号相位抖动估计值；(c)补偿前后回波去斜信号波形

Fig.5　Time-domain waveforms of dechirped signals and phase noise estimates. (a) Reference dechirped signal and echo dechirped signal; (b) Phase noise estimates of the reference dechirped signal; (c) Waveforms of the echo dechirped signal before and after compensation

为定量评估回波去斜信号相位噪声的补偿效果，本文从两个关键维度展开分析：一是对比补偿前后回波去斜信号的半周期宽度稳定性，二是分析其相位噪声特性，并引入等相位间隔采样法处理后的信号作为参照组进行横向对比，相关结果如图6所示。图6(a)呈现了连续240次半周期宽度的估计结果。由图可知，采用去偏斜滤波方法完成相位噪声补偿后，回波去斜信号的半周期宽度稳定性显著提升。具体数据显示：补偿前，半周期宽度的标准差为0.54 ns；经等相位间隔采样法补偿后，该标准差降至约0.24 ns；而通过去偏斜滤波方法补偿后，标准差进一步减小至0.15 ns，相较于补偿前，稳定性提升了3.6倍。图6(b)为补偿前后回波去斜信号的相位噪声曲线。分析可见，在频偏小于10 kHz的频段内，去偏斜滤波方法对相位噪声的抑制效果明显优于等相位间隔采样法，处理后信号的相位噪声水平更低。

最后，为进一步评估相位噪声补偿对回波去斜信号的影响，对补偿前后的信号开展时频分析，分别得到如图7(a)（补偿前）与图7(b)（补偿后）所示的距离像结果。从图中可直观观察到，经相位噪声补偿后，雷达系统的距离分辨力显著提升：一方面，补偿后的距离像中目标能量更趋集中，直接体现出雷达对目标位置的

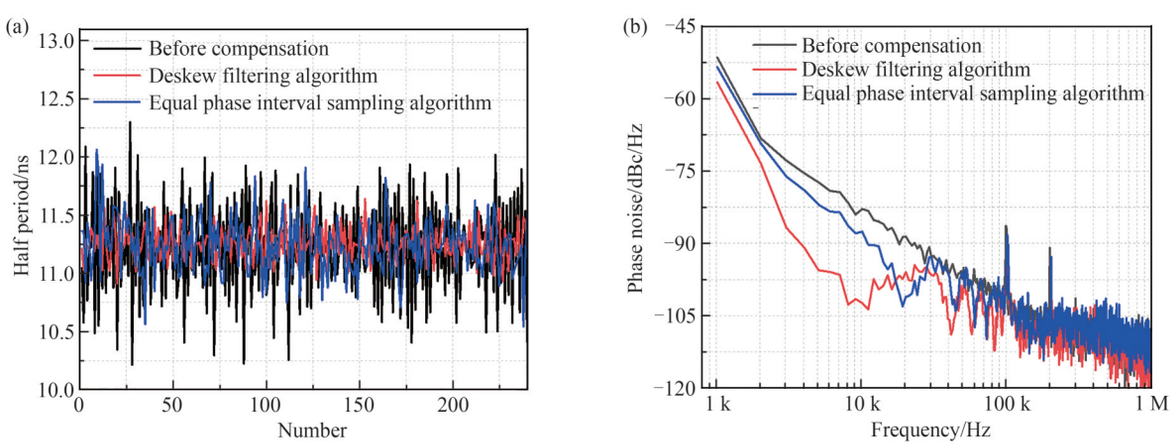


图6　补偿前后回波去斜信号的相位稳定性。(a)半周期宽度；(b)相位噪声

Fig.6　Phase stability of the echo dechirped signals before and after compensation. (a) Half-period width; (b) Phase noise

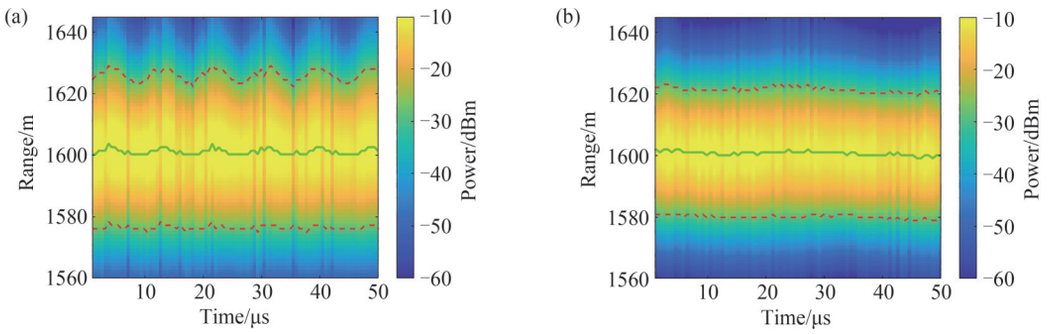


图7 补偿前后距离像。(a)补偿前的距离像;(b)补偿后的距离像

Fig.7 Range profile with and without compensation. (a) Range profile without compensation; (b) Range profile with compensation

分辨能力增强;另一方面,距离测量结果的偏差范围得到有效抑制,具体表现为补偿后距离像中目标位置的波动幅度明显减小。为定量验证去偏斜滤波方法对距离分辨力及测距稳定性的提升效果,我们在图7的距离像中进行了针对性标注:以红色虚线标出10 dB带宽对应的距离范围,以绿色曲线标注各时刻的距离测量值。经计算可知,10 dB带宽的距离差从补偿前的49.57 m降至补偿后的41.28 m,距离测量结果的标准差也从补偿前的0.97 m降至补偿后的0.78 m。上述定量与定性结果均表明,去偏斜滤波方法可有效改善雷达系统的距离分辨力与测距稳定性。

3 结论

本文针对微波光子FMCW雷达中相位噪声制约其宽带性能充分发挥这一问题展开研究,提出基于去偏斜滤波的微波光子FMCW雷达相位噪声补偿方法,采用光四倍频结构提升距离分辨率,增加参考延时和混频支路获取参考去斜信号,结合去偏斜滤波算法补偿回波去斜信号的相位抖动。搭建实验系统,验证了微波光子四倍频功能,生成了频率范围20~20.4 GHz的四倍频信号。经去偏斜滤波算法处理后,回波去斜信号半周期稳定性提高3.6倍,相位噪声得到有效抑制,距离像中目标能量更集中,测距精度和分辨率显著提升,充分验证去偏斜滤波方法在抑制微波光子雷达相位噪声方面的有效性。

参考文献

[1] LI Weitao, XIONG Yuyong, HONG Sicheng, et al. Wide range and accurate displacement measurement technique using FMCW radar[J]. IEEE Microwave and Wireless Technology Letters, 2025, 35(4): 492-495.

[2] ROUCA A, PEREIRA A, FILIPE A D, et al. Accurate through-wall breathing rate measurements using a C-band FMCW radar[J]. IEEE Sensors Journal, 2025, 25(7): 12097-12108.

[3] LIU Xuyang, MAKTOOMI M H, ALESHEIKH M, et al. A 49-63 GHz phase-locked FMCW radar transceiver for high resolution applications[C]. ESSCIRC, 2023: 509-512.

[4] YU Yingrui, JIANG Zhihao, ZHANG Hui, et al. A low-profile beamforming patch array with a cosecant fourth power pattern for millimeter-wave synthetic aperture radar applications[J]. IEEE Transactions on Antennas and Propagation, 2020, 68(9): 6486-6496.

[5] SERAFINO G, SCOTTI F, LEMBO L, et al. Toward a new generation of radar systems based on microwave photonic technologies[J]. Journal of Lightwave Technology, 2019, 37(2): 643-650.

[6] CLARK T, WATERHOUSE R. Photonics for RF front ends[J]. IEEE Microwave Magazine, 2011, 12(3): 87-95.

[7] GUO Qingshui, ZHANG Fangzheng, WANG Ziqian, et al. High-resolution and real-time inverse synthetic aperture imaging based on a broadband microwave photonic radar[C]. MWP, 2017: 1-3.

[8] WANG Yaochen, PHELPS T, RUPAJULA B, et al. 64 GHz 5G-based phased-arrays for UAV detection and automotive traffic-monitoring radars[C]. PAST, 2019: 1-4.

[9] LAGHEZZA F, SCOTTI F, ONORI D, et al. ISAR imaging of non-cooperative targets via dual band photonics-based radar system[C]. IRS, 2016: 1-4.

[10] ZHANG Fangzheng, GUO Qingshui, WANG Ziqian, et al. Photonics-based broadband radar for high-resolution and real-time inverse synthetic aperture imaging[J]. Optics Express, 2017, 25(14): 16274.

[11] PENG Shaowen, LI Shangyuan, XUE Xiaoxiao, et al. High-resolution W-band ISAR imaging system utilizing a logic-operation-based photonic digital-to-analog converter[J]. Optics Express, 2018, 26(2): 1978.

[12] MA Cong, WANG Xiangchuan, DING Zeyong, et al. High-resolution microwave photonic sparse imaging radar[J].

IEEE Transactions on Microwave Theory and Techniques: 1-11.
[13] GAO Bindong, ZHANG Fangzheng, ZHAO Ermao, et al. High-resolution phased array radar imaging by photonics-based broadband digital beamforming[J]. Optics Express, 2019, 27(9): 13194.
[14] SUN Yu, ZHU Dan, DING Jiewen, et al. Dual-band microwave photonic imaging radar based on optical frequency combs and polarization multiplexing[C]. IPOC, 2024: 1-3.
[15] JIANG Tianyu, RUBULS K, JOHARIFAR M, et al. Photonics-enabled 6G distributed MIMO: experimental study in an indoor environment[C]. MWP, 2024: 1-5.
[16] GOLDMAN S J. Phase noise analysis in radar systems using personal computers[M]. Hoboken, NJ, USA: Wiley, 1989.
[17] WU Kan, OUYANG Chunmei, WONG Jiahaur, et al. Frequency response of the noise conversion from relative intensity noise to phase noise in the photodetection of an optical pulse train[J]. IEEE Photonics Technology Letters, 2011, 23(8): 468-470.
[18] SHI Jingzhan, WANG Yian, ZHU Dan, et al. A microwave photonic FMCW radar with suppressed phase noise based on equal phase interval sampling[J]. IEEE Photonics Technology Letters, 2025, 37(4): 195-198.
[19] RENUKA B, SINGH M. Phase noise reduction in optoelectronic oscillator with quadratic fiber bragg grating dispersion engineering[J]. IEEE Transactions on Instrumentation and Measurement, 2025, 74: 1-7.
[20] META A, HOOGEBOOM P, LIGTHART L P. Range non-linearities correction in FMCW SAR[C]. IGARSS, 2006: 403-406.
[21] PEEK K. Estimation and compensation of frequency sweep nonlinearity in FMCW radar[D]. University of Twente, 2011.
[22] DING Zhenyang, YAO X S, LIU Tiegen, et al. Compensation of laser frequency tuning nonlinearity of a long range OFDR using deskew filter[J]. Optics Express, 2013, 21(3): 3826-3834.
[23] CEN Qizhuag, DAI Yitang, YIN Feifei, et al. Low phase noise linearly chirped microwave pulse based on opto-electronic oscillator[C]. MWP, 2016: 102-105.
[24] ZHANG Xiangpeng, ZENG Henan, YANG Jiyao, et al. Novel RF-source-free reconfigurable microwave photonic radar[J]. Optics Express, 2020, 28(9): 13650.
[25] LIU Mingzhen, LIU Shifeng, ZHU Nan, et al. Low phase noise wideband LFM signal generation by injection-locking an optoelectronic oscillator[C]. OECC, 2021: 1-3.
[26] XUE Zhujun, LI Shangyuan, LI Jiading, et al. OFDM radar and communication joint system using opto-electronic oscillator with phase noise degradation analysis and mitigation[J]. Journal of Lightwave Technology, 2022, 40(13): 4101-4109.
[27] KRUSE S, SHROFF V S, BAHMANIAN M, et al. An ultra low phase noise frequency synthesizer with optical output for 77 GHz photonic radar[C].GeMiC, 2025: 148-151.
[28] DUAN Shaochen, MO Baohang, WANG Xudong, et al. Photonic-assisted regenerative microwave frequency divider with a tunable division factor[J]. Journal of Lightwave Technology, 2020, 38(19): 5509-5516.
[29] KITTLAUS E A, ELIYAHU D, GANJI S, et al. A low-noise photonic heterodyne synthesizer and its application to millimeter-wave radar[J]. Nature Communications, 2021, 12(1): 4397.

Phase Noise Suppression System for Microwave Photonic FMCW Radar Based on Deskew Filtering

ZHU Jintao, SHI Jingzhan, ZHU Dan, LIU Qiang, LIN Dongdong,
ZHANG Na, GAO Bindong, WANG Yiping
(*Nanjing Normal University, School of Computer and Electronic Information, Ministry of Education Key Laboratory of NSLSCS, Nanjing* 210023, *China*)

Abstract: Frequency-Modulated Continuous-Wave (FMCW) radar is widely used in military, autonomous driving, and other fields for its high resolution, low power consumption, and strong anti-interference. However, traditional microwave electronic radars fail to meet broadband signal generation/processing needs, leading to the development of microwave photonic radar. By combining photonics and electronics, it overcomes the "electronic bottleneck," with optical frequency multiplication and dechirping reception architectures gaining attention for large bandwidth and simple structure. Nevertheless, in this architecture, frequency multiplication degrades phase noise (by 20 $\log_{10}(n)$ dB for multiplication factor n), while electro-optic/optoelectronic conversion worsens it. Phase noise impairs radar accuracy, resolution,

and anti-interference, limiting broadband advantages. Existing suppression technologies for microwave photonic radar often suffer from complexity, high cost, or new noise introduction, demanding more effective compensation.

This paper proposes a phase noise compensation scheme for microwave photonic FMCW radar using deskew filtering. The system adopts an optical quadrupling structure (boosting distance resolution) plus reference delay and mixing branches. The baseband linear frequency-modulated (LFM) signal splits into two paths: one drives the microwave photonic quadrupling module to generate a transmitted signal (4× baseband frequency/bandwidth, 4× phase noise), whose echo is processed via a microwave photonic mixer to get an echo dechirped signal with phase jitter; the other undergoes reference delay/mixing to produce a reference dechirped signal. Deskew filtering compensates the echo dechirped signal as follows: apply Hilbert transforms to both signals for complex signals, estimate phase noise via the reference, remove phase noise′s delay dependence in the echo using the deskew filter, and eliminate phase noise to mitigate radar performance impacts.

An experimental setup was built to verify the feasibility of the proposed scheme. The initial frequency of the baseband linear frequency-modulated signal was 5 GHz, with a bandwidth of 100 MHz. After passing through the microwave photonic quadrupling module, a quadrupled frequency signal in the range of 20～20.4 GHz was generated, effectively expanding the bandwidth. The reference and echo dechirped signals were collected and processed using the deskew filtering algorithm. To evaluate the effectiveness of phase noise compensation in the dechirped echo signal, we analyze two key aspects: first, comparing the stability of the half-period of the dechirped echo signal before and after compensation, and second, examining its phase noise characteristics. A reference group processed using the equal phase interval sampling method was introduced for comparative analysis. The results show that before compensation, the standard deviation of the half-period was 0.54 ns. After compensation with the equal phase interval sampling method, this value decreased to approximately 0.24 ns. Further compensation using the deskew filtering method reduced the standard deviation to 0.15 ns, representing a 3.6 times improvement in stability compared to the pre-compensation state. This indicates that the phase noise compensation achieved through the deskew filtering method significantly enhances the stability of the half-period of the dechirped echo signal. Regarding phase noise characteristics, the experimental results demonstrate that within the frequency offset range of less than 10 kHz, the deskew filtering method outperforms the equal phase interval sampling method in suppressing phase noise, resulting in a lower phase noise level in the processed signal. Additionally, a time-frequency analysis was conducted on the signals before and after compensation to compare the range profiles. The results reveal that the target energy in the compensated range profile becomes more concentrated, and the deviation range of the distance measurement results is effectively suppressed. Specifically, the distance corresponding to 10 dB bandwidth decreased from 49.57 m (pre-compensation) to 41.28 m (post-compensation), while the standard deviation of distance measurement results reduced from 0.97 m (pre-compensation) to 0.78 m (post-compensation). Collectively, these findings demonstrate that the deskew filtering method effectively improves the range resolution and distance measurement stability of the radar system.

Key words: Microwave photonic frequency multiplication; Frequency-modulated continuous wave radar; Phase noise; Deskew filtering; Phase noise compensation

OCIS Codes: 060.5625; 280.5600

CSTR: 32255.14.gzxb20265503.0355113

Foundation item: National Natural Science Foundation of China (62575140, 62101269, 62501291, 62405139, 62401268, 62505139), National Key Research and Development Program of China Young Elite Scientists Sponsorship Program by CAST (2022QNRC001), Open Project from Key Laboratory of Radar Imaging and Microwave Photonics (Nanjing University of Aeronautics and Astronautics), Ministry of Education (NJ20210007), Natural Science Foundation of the Jiangsu Higher Education Institutions of China (24KJB510014)